

A NEW HEURISTIC DECISION TREE AND TIME-INVARIANT DETECTION OF PADDY GROWTH STAGES FROM MODIS DATA

¹S. MULYONO, ²M. SADLY, ¹M. IVAN FANANY, ¹T. BASARUDDIN

¹Faculty of Computer Science, Universitas Indonesia, Indonesia

²Indonesia Agency for Assessment and Application of Technology, Indonesia

E-mail: sidikm@gmail.com, muhamad.sadly@bppt.go.id, ivan@cs.ui.ac.id, chan@cs.ui.ac.id

ABSTRACT

Satellite remote sensing has essentially been applied in agriculture such as monitoring paddy growth stages, cropping schedule, and fertilizer management over vast areas. Many methods have been devoted for detecting paddy growth stages by deriving a certain profiles of vegetation indices from high temporal resolution satellite data. In this paper, we introduce a time-variant method referred to as a heuristic decision tree (HDT) for detecting 3-classes of paddy growth stages from a limited number of MODIS images and generalize the result through machine learning to predict the growth stages in time-invariant manner. We compared our proposed method to two previous studies in [8] and [9]. For the time-variant case, all methods are validated by 124 times of observation data among 50 reference points from field survey. After doing some adjustments for calculating the accuracy, the result shows that the accuracy for [8, 9], and our proposed method are 0.8951, 0.9375, and 0.9435 respectively. For the time-invariant case, we evaluate three Kernel-based Regularized (KR) classification methods, i.e. Principal Component Regression (KR-PCR), Extreme Learning Machine (KR-ELM), and Support Vector Machine with radial basis function (RBF-SVM). All data samples are divided into training (25%) and testing (75%) sampling, and all models are trained and tested through 10-rounds random bootstrap re-sampling method to obtain more variety on hypothesis models during learning. The best model for each classifier method is defined as the one with the highest kappa coefficient during testing. The experimental results for 3-classes of paddy growth stages prediction show that the classification accuracy in testing for our proposed method of each learner are 0.8485, 0.8874, and 0.8252 respectively, whereas for previous study [8] are 0.6845, 0.7845, and 0.6949 respectively.

Keywords: *Remote sensing, MODIS, Phenology, Paddy growth stages, Kernel based learner*

1. INTRODUCTION

Rice is one primary staple foods for more than two hundred million people in Indonesia. To ensure national food security, Indonesian government needs to forecast national rice stock periodically. Thus accurately detecting current paddy growth stages is paramount. The anomalous phenomena such as drought, flood, pests, insects and diseases attacks always threaten every moment. They may increase the risk of crop failure if early warning and mitigation system are not timely announced.

In Indonesia, paddy may be planted 2 or 3 times a year for a certain cultivar in irrigated sites, and once a year in rain-fed site. The cycles show a number of periodic waves of the phenology profile a year-around. Each cycle characterizes paddy's unique profile, which begins from planting stage, followed by heading stage, and ending at harvesting

stage. It varies depending on cultivar and planting area, and heavily influenced by surrounding environment conditions. The cycles represent not only information on irrigation schedule or fertilizer management [3], but also help in understanding the response of agriculture to global changes (such as drought and flood events). In addition, the cycles also provide references for future food production [3] and may indicate pest and diseases attacks that can be used to minimize future crop failure.

Paddy plantation, however, is constrained not only by some physical factors (such as air temperature, soil, and climate), but also by irrigation schedule and arbitrary decisions (local wisdom) of the farmers. In the case of rain-fed paddy fields, the farmers also sometimes switch paddy crop with other economically more valuable crops such as peanuts, cassavas, soybeans, and other short-lived crops depending on climate

condition and market demands. As a consequence, such decisions cause complex cropping patterns, which means spatial crop rotation may change arbitrarily in every planting season. Meanwhile, widely used statistical estimation of rice production, which is largely based on direct human observation, often limited in terms of field of view and variation details that can be seen by naked eyes. To cope with this limitation, human observers tend to over-generalize thus causes excessive or over-estimated prediction. More reliable and rapid harvest yield estimation for paddy fields is a critical success factor to support national food security program. In fact, it also needs an accurate and timely rice monitoring and rapid rice harvest area estimation [1, 2].

2. RELATED WORKS

Many studies predict paddy phenology using remote sensing data. Time-series of various vegetation indices derived from MODIS images, including Normalized Difference Vegetation Index (NDVI), Normalized Difference Soil Index (NDSI), Enhanced Vegetation Index (EVI), and Land Surface Water Index (LSWI) have effectively been applied for large scale mapping of flooding and transplanting paddy rice in summer season [4]. The algorithm maps paddy rice fields in 13 countries of South and Southeast Asia [5]. The MODIS based approach for paddy rice detection and mapping is extended and adapted [6], as used in [5], with more variables, mixed and local rice cropping systems, including single, early, and late rice. This algorithm is further improved [7] by developing the variable threshold model (T) in conjunction with MODIS EVI using Synthetic Aperture Radar (SAR)-based irrigated paddy field maps.

Three procedures for determining paddy growth stages are as follows [8]: (i) prescription on constraining multi-temporal MODIS data; (ii) filtering time-series EVI profile by time-frequency analysis; and (iii) specifying the phenological stages by detecting the maximum point, minimum point, and inflection point from the smoothed time-based EVI profile. Based on these procedures, paddy growth stages are characterized by three dates, (a) heading date, characterized by the maximum point of EVI time profile, (b) flooding and planting date, indicated by the minimum point of EVI time profile and the first derivative changes from negative to positive, and (c) harvesting date, presented by the minimum point of first derivative. Meanwhile, LSWI and EVI combination are also used to provide sensitivity to current water during

flooding and transplanting date. However, the relationship between EVI and LSWI may become complicated [7] due to the growth of aquatic plants during flooding and transplanting date. Therefore, the detection of this date is simplified in [4] by using a global threshold value of 0.05 constrained by $LSWI + 0.05 \geq EVI$ to detect flooding and transplanting date.

Based on three dates proposed in [8], a simple algorithm [9] was proposed by defining the threshold values of EVI and LSWI derived from MODIS 500-m in each stage. The algorithm can detect 3-classes of paddy growth stages with complex cropping pattern. Another approach [18] proposed the threshold value of EVI and NDWI to estimate rice planting time with complex cropping pattern. A comparative study [10] presented satellite and model based crop phenology in West Africa. The model used 4 dates EVI phenology crops, i.e. green-up or start of season (SOS); maturity or start of maximum (SMAX), senescence or end of maximum (EMAX), and dormancy or end of season (EOS).

Cloud cover and atmospheric condition cause some noises on time-based phenology profiles constructed from remote sensing data. Further analysis should apply some filtering and smoothing process. Time-based EVI profile analysis used wavelet and Fourier transforms to remove the noise by dividing the noise components and reconstructing the desired profile [9, 12]. A progressive iteration approximation (PIA) provides a Bézier curve [12], or Savitzky-Golay filter [19] can also be used for signal smoothing and reducing noise representation in time-based NDVI profile. A cubic interpolation method [3] on discrete NDVI points obtains a smoothed NDVI curve and calculates its slope. A comprehensive analysis [19] compared the capability and reliability of four models (double logistic, Fourier, asymmetric Gaussian, and Whittaker) for smoothing temporal satellite sensor observations with the purpose of estimating phenological parameter of onset of greenness (OG).

In contrast with other approaches in rice phenology prediction, a method proposed in [20] stored the calculated one-year time-series NDVI derived from MODIS into one scene of 8-day composite with 46 bands. After wavelet-based smoothing process, an artificial neural network algorithm learned to detect 3-classes of rice cropping patterns and 3-classes of non-rice crop objects in South Asia. The study was further extended [21] by using intrinsic mode function



(IMF) obtained from the empirical mode decomposition (EMD) to mask out non-rice cropped area. Based on the smooth EVI time-series data derived from a low-pass filter, the method classified 4-types rice cropping patterns in Mekong Delta, Vietnam.

Many previous researches have successfully utilized various time-based vegetation indices derived from various remote sensing data to determine paddy crop phenological stages. To have a better-smoothed paddy phenology profile, they have to employ high temporal resolution (many time-series) of remote sensing images. Such time-series data requires an enormous computer memory and storage, especially for predicting the existing paddy growth condition in a wide coverage area.

The threshold specification algorithms proposed by previous studies should be improved to define a finer date time ranges in wide coverage area by incorporating other parameters. This paper addresses the following main issues on: (i) how to define the date of paddy phenological growth stages in simpler, more reliable way, and more accurate; (ii) how to determine the current paddy growth stages using only some limited series of temporal resolution of remote sensing data, and (iii) how to realize a general prediction model derived from this limited series that is applicable in time-invariant manner for detecting 3-classes of paddy growth stages at any given time with high accuracy. Instead of relying on time-series data, we pursue a spectral-based time-invariant prediction model.

This paper addresses these three issues by focusing on utilizing the spectral properties of remote sensing images instead of relying on time series or temporal images. Initially, we construct the paddy crop time-based phenology profiles from a limited six-year time series of EVI and LSWI derived from MODIS. We then construct an algorithm for indicating three-labeled paddy growth stages, which contain the LSWI threshold to detect water existence, and EVI threshold to detect greenness level. The results of our algorithm have been validated by 124 times of observation data among 50 monitoring sites of field survey held during June-September 2012 laid around Karawang and Indramayu district of West Java Indonesia. The results showed that paddy growth stages detected by using this algorithm matched field survey data. Therefore, they can be considered as ground reference data for further analysis.

Henceforward, regardless of the prediction time, paddy growth stages prediction models are

constructed from six-band spectral of MODIS using three Kernel-based Regularized (KR) classification methods, i.e. Principal Component Regression (KR-PCR), Extreme Learning Machine (KR-ELM), and Support Vector Machine with radial basis function (RBF-SVM). About 25% of data samples are for training, and the other 75% are for testing. All models are trained and tested through 10-round random bootstrap re-sampling methods to obtain more variety on hypothesis models. The best model for each classifier is the one that has the highest kappa coefficient during testing.

Among the previous studies, to the best of our knowledge, only two studies proposed prediction models for detecting paddy growth stages.

The first study [8] used one-year time-based EVI profile derived from MODIS satellite. After smoothing process using wavelet and Fourier transforms, this method calculates the first and second derivative of EVI for detecting maximum and minimum value to distinguish heading date and flooding & planting dates. No reports, however, on how this method works in case of paddy field with complex cropping patterns.

The second study [9] proposed algorithm for detecting paddy growth stages similar to [8]. Since paddy fields have complex cropping patterns, the algorithm incorporates LSWI [9] in determining the flooding date. The algorithm also uses global threshold of 0.05 to release the greenness effect caused by aquatic plants that usually grow while water flooding in the paddy field, as proposed in [4].

In this paper, we compare the effectiveness of our method to these two previous approaches. We also construct prediction model for three-labeled paddy growth stages defined by [8].

3. DATA SAMPLES

We conducted a field campaign for paddy growth stages observation during June - October 2012 around Karawang and Indramayu Districts, lying in the Northern part of West Java-Indonesia. Figure 1 shows the study area, which comprises 2 locations. The first is located in Karawang district that has 24 sites with 3-times observation, and the second is located in Indramayu district that has 26 sites with 2-times observation. In total, we have 124 times observation. In general, the rice planting pattern in these locations consists of three period of planting: (a) wet season planting (November – February), (b) First dry season planting (March – June), and (c) Second dry season planting (July – October).

Nevertheless, no guarantee that the farmers do planting simultaneously and follow a same schedule since each paddy field has different irrigation schedule. In addition, sometimes farmers have also to change the schedule due to pests, insects, and diseases attacks. In other cases, the farmers have to change paddy crops with other stronger or more valuable crops such as peanuts, cassavas, soy beans, depending on climate condition and market demands. These factors have led to complex cropping pattern and opened great challenges to develop a more effective remote sensing procedures that are applicable on solving agricultural problems.

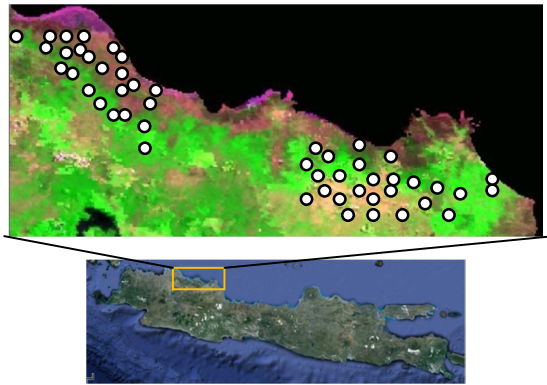


Figure 1: Area Of Study Laid On Karawang And Indramayu District Of West Java

A series of 8-day composite MODIS images used in this study are taken during January 2008 - July 2014. We processed MODIS surface reflectance product computed from the MODIS bands 1, 2, 3, 4, 5, 6, and 7 (centered at 648 nm, 858 nm, 470 nm, 555 nm, 1240 nm, 1640 nm, and 2130 nm, respectively) with 500 meter spatial resolution, and all images were also preprocessed in two stages for geometric and atmospheric corrections. In this study, we neglected band 5 of MODIS due to an error caused by its sensor, and used the rest of six bands for analysis.

From these data, we derive time series of EVI and LSWI using equation (1) and (2),

$$EVI = 2.5 \frac{R_{NIR} - R_{Red}}{R_{NIR} + R_{Red} - 7.5R_{Blue} + 1} \quad (1)$$

$$LSWI = \frac{R_{NIR} - R_{SWIR}}{R_{NIR} + R_{SWIR}} \quad (2)$$

where R_{Blue} , R_{Red} , R_{NIR} , R_{SWIR} are surface reflectance value from blue, red, near infrared, and short wave infrared band of MODIS respectively.

3. METHODOLOGY

3.1. The Algorithm For Detecting Paddy Growth Stages

In this paper, our algorithm divides paddy growth stages into three dates, i.e., (1) flooding & planting date; (2) heading & harvesting date; (3) post-harvest date. Hereinafter, these dates are indicated by index 1, 2, and 3 respectively. We use a global threshold value of 0.06 using $LSWI + 0.06 \geq EVI$ approach to distinguish between flooding & transplanting stage and heading stage to reduce the greenness effect of aquatic plants that usually grow when the water inundated paddy field. We define three dates of paddy growth stages as follows:

(a) Flooding & planting stage

In contrast with other crops and other dynamic objects, the paddy field is unique that it has plowed and flooded period by water before rice planting, where the greenness level is located closed to the minimum point of EVI profile, indicated by $LSWI + 0.06 \geq EVI$.

(b) Heading and harvesting stage

Heading stage starts with flowering event before senescent of leaves, which is indicated by increasing of greenness level to the maximum point of EVI and constrained by $LSWI + 0.06 \leq EVI$. Meanwhile, harvesting stage starts while the individual grain is mature, fully developed, hard, and has 100 percent of the filled grains turned yellow. The point closed to minimum value of first derivative marks this stage, which means the second derivative value is closed to zero, or EVI value is closed to 0.28. In contrast with [8] and [9], since harvesting event is timely too sort, and may be found rarely among a series of 8-day composite MODIS images, so we combined it with heading date.

(c) Post-harvest stage

This stage that was not defined by [8] and [9], is a phase before plowing, where the rice shoots will grow back from the base of rice plants that have been harvested. In addition, wild weeds may also grow and flourish due to supply of water and nutrients remained in the soil. When the rain fell and flooded the rice fields, then this condition will be similar to the planting stage. This stage will start from $LSWI + 0.06 \leq EVI$ until $LSWI + 0.06$ value is closed to EVI , while the second derivative value change to positive or EVI value is less than 0.28.

Figure 2 illustrates the position of each paddy growth stage associated with time based EVI profile, where the green, blue, red, and violet solid lines indicate time-based EVI profile, time-based LSWI profile, first derivative of EVI profile, and second derivative of EVI profile respectively. We propose a HDT for detecting three dates of paddy growth stages as shown in figure 3. From this view of point, we can derive spectral data samples from all sites as referred by spectral library for each growth stage using this algorithm for building classifiers with three Kernel-based Regularized (KR) classification methods.

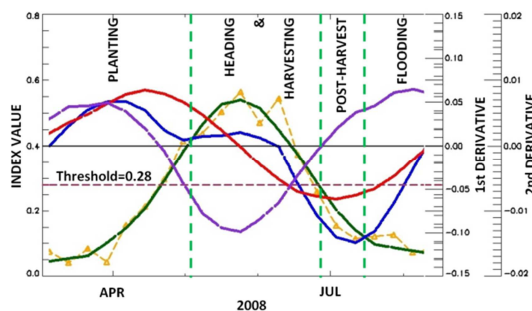


Figure 2: New Definition Of Paddy Phenological Stages Using Time-Based EVI Profile

Instead of using previous paddy growing dates, actually we used another terminology of dates that commonly used by most farmers during field campaign, i.e. plowing, first vegetative, second vegetative, generative, harvested and bare land, (hereinafter indicated by A, B, and C respectively). However, for validation purpose, these terminologies of date have to be adjusted with terminologies used in previous methods [8], [9]. The adjustments of date terminology between field campaign and each method are shown in table 1 and 2. Based on these adjustments, in the result session, we calculate the accuracy of each algorithm using the confusion matrix with size 3x3 for our proposed method, and 2x2 for previous studies.

For learning the classifiers, all paddy growth stages detected by this algorithm using MODIS data are divided into train and test samples as shown in table 3. Moreover, these train samples are divided again into 25% for learning and 75% for validation during learning through 10-rounds random bootstrap re-sampling method to obtain more variety on hypothesis models. We intentionally set-up number of data sample for testing much more than training, in order to prove the generalization ability of the models constructed from learning process. Moreover, the best model

for each classifier method is the one that has the highest kappa coefficient during testing.

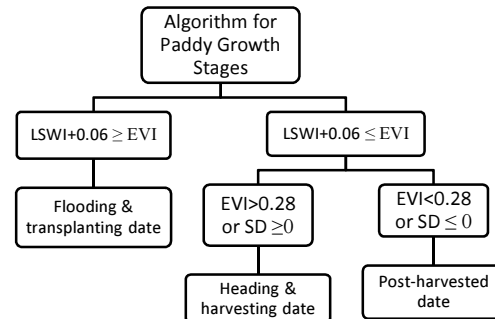


Figure 3: A Heuristic Decision Tree (HDT) For Detecting Three Dates Of Paddy Growth Stages

Table 1: The Adjustment Dates Between Field Campaign And Our Proposed Algorithm

Dates used in Algorithm	Dates used in field campaign
1. Flooding and transplanting date	Plowing date (A) 1st vegetative date (A)
2. Heading & harvesting date	2nd vegetative date (B) Generative date (B)
3. Post-harvest date	Harvested and bare land date (C)

Table 2: The Adjustment Dates Between Field Campaign And Algorithm Proposed by [8] and [9]

Dates used in Algorithm	Dates used in field campaign
1. Flooding and transplanting date	Plowing date (A) 1st vegetative date (A) Harvested and bare land date (C)
2. Heading date	2nd vegetative date (B)
3. Harvesting date	Generative date (B)

Table 3: Data Samples

No	Class	Number of samples		
		Train	Test	Total
1	Flooding & planting	500	5,724	6,224
2	Heading & harvesting	500	4,392	4,892
3	Post-harvest	500	2,616	3,116

3.2 Kernel-based Classification Method

Support vector machines (SVM) is a popular machine learning technique for data classification. Basically, SVM classifies data by determining the separating hyper-plane or decision surface, which maximizes the margin between the two classes in the training data [13]. One major disadvantage, however, is that SVM classification is binary. This problem can be resolved in a simple and robust



procedure by training several SVMs simultaneously in any multiclass approaches. Kernel function provides SVMs with a powerful ability of efficiently determining the nonlinear decision surfaces after transforming the input space into kernel space. In addition, SVM is theoretically able to transform a non-convex problem into a convex problem with a single global minimum thanks to its quadratic optimization scheme. Given a training set of instance-label pairs $(x_i, y_i), i = 1, \dots, l$, where $x_i \in R^n$ and $y \in \{1, -1\}^l$, the SVM requires the solution of the following optimization problem:

$$\begin{aligned} \min_{w,b,\xi} \quad & \frac{1}{2} w^T w + C \sum_{i=1}^l \xi_i \\ \text{Subject to} \quad & y_i (w^T \phi(x_i) + b) \geq 1 - \xi_i \\ & \xi_i \geq 0 \end{aligned} \quad (1)$$

Here the training vectors x_i are mapped into a higher dimensional space by the function ϕ . SVM finds a linear separating hyperplane with the maximal margin in this higher dimensional space, whereas $C > 0$ is the penalty parameter of the error term.

The development of SVMs classification for paddy growth stages is done using a library for support vector machines (LIBSVM), which is based on sequence minimal optimization (SMO) [14]. This library was integrated into Interactive Data Language (IDL) program for linking to the data samples. The kernel trick used in this paper is radial a basis function

$$K(x_i, x_j) = \exp(-\gamma \|x_i - x_j\|^2), \gamma > 0 \quad (2)$$

Compared to other kernel tricks (linear, polynomial, and sigmoid), the γ parameter of RBF kernel provides greater flexibility in controlling the desired classification accuracy. Such accuracy control mechanism is highly important when we want to combine the SVM as weak classifiers in a boosting ensemble framework to overcome the over-fitting problem.

Principal component regression (PCR) is a regression analysis that uses the principal component analysis (PCA) to estimate regression coefficients. The PCR overcomes problems that arise when the independent variables are closed to being collinear. In PCR, the role of the independent variables, which are directly used in common regression on the dependent variable, is replaced by the principal components of the independent variables. The basic idea in PCR is that after choosing a set of suitable PCs that are indexed g , the input features of X have been retained by score

matrix V_g [15] and then perform a multiple linear regression (MLR) with V_g instead of X for $n \times m$ calibration data matrix Y

$$y = V_g \beta + \epsilon \quad (3)$$

where in this paper, y is related to (i) the output vector in term of regression, and (ii) the output matrix of labeled classification in binary code [-1,1]. The least squares method then gives coefficient of regression

$$\hat{\beta} = V_g^T (V_g^T V_g)^{-1} y \quad (4)$$

So in the development of prediction models using PCR, the most decisive factors are only the score matrix V_g and coefficient of regression $\hat{\beta}$. Finally the parameters of the model are computed for the selected PC. Consider a new sample z and predicted value by \hat{y} (both uncentered), and let \bar{x} and \bar{y} be the mean value of calibration samples. By improving equation (3) then the prediction for new sample h takes the form.

$$\hat{y} = \bar{y} + (h - \bar{x}) V_g \hat{\beta} \quad (5)$$

Meanwhile, ELM originally developed by [16], is a generalization of the single-hidden-layer feed forward neural networks (SLFNs), where all the parameter of networks do not need to be updated iteratively. The ELM randomly chooses instead a number of hidden nodes and analytically determines the output weights of SLFNs, so that it can learn extremely faster than traditional SLFNs. The decision function of ELM with n hidden nodes can be expressed as

$$f(x) = \sum_{i=1}^n \beta_i g_i(x), \quad x \in R^d, \beta_i \in R \quad (6)$$

where $g_i(x)$ is the hidden layer output corresponds to the input samples x . The β_i is the output weight vector between hidden layer output and the network output. In this paper, we apply Radial Basis Function (RBF) as a hidden nodes function, which defined as

$$g_i(x) = g(b_i \|x - a_i\|), a_i \in R^d, b_i \in R^+ \quad (7)$$

where a_i and b_i are the center and impact factor of the i th hidden nodes respectively. Equation (1) can be written in matrix form as

$$F = G\beta \quad (8)$$

If the number of hidden layer is equal to the number of training samples, the equation (8) can be easily resolved by using conventional least square method. However, in most cases the number of



hidden nodes is much less than the number of training samples, then this problem can be accomplished by

$$\beta = G^T(G^T G)^{-1}F \quad (9)$$

Compared to equation (4), the equation (9) has the same form of pseudo inverse matrix, which called as the Moore-Penrose generalized inverse of matrix.

As the SVM, for better generalization performance of PCR and ELM, we regularize our machine learning based on ridge regression [17], which adding a positive value I/C as a penalty into regression coefficient in equation (4) and (9). By minimizing errors of both equations, the solution to the ridge regression problem is given. Furthermore, by defining a RBF kernel matrix (2), therefore the decision function for PCR and ELM can be written in equation (10) and (11) respectively.

$$f(x) = K(h, v) \left(\frac{I}{C} + K(v_i, v_j) \right)^{-1} y \quad (10)$$

$$F(x) = K(g(h), g) \left(\frac{I}{C} + K(g_i, g_j) \right)^{-1} y \quad (11)$$

Here parameter C and γ of each base learner for classification must be defined in advanced by using grid-search technique, and the best parameters are shown in table 4.

3.3. Savitzky-Golay Filter, First Derivative, And Second Derivative

Savitzky-Golay filter defined as a weighted moving average with weighting given as a polynomial of a certain degree. It is applied to time-based EVI profiles for the purpose of smoothing the profile without greatly distorting the signal. This is done by fitting successive sub-sets of adjacent data $2m + 1$ points of EVI profiles with a low-degree polynomial p ($p \leq 2m$) by the method of linear least squares [22], which in a process known as convolution. The advantage of the Savitzky-Golay filter is that it tends to preserve certain features of the time-series like local minima and maxima and works especially well when the typical peaks of the signal are narrow, while the heights and widths of the curves are generally preserved. Since it uses a certain degree of polynomial function, then the first derivative and second derivative can be easily computed parallel with smoothing process. All filtering, first derivation, and second derivation processes are done by constructing program coding in interactive data language (IDL).

Table 4: The Best Learning Parameters

Data source	Base learner	Parameter γ	Parameter C
Sakamoto	RK-PCR	64	2
	RK-ELM	4	128
	RBF-SVM	64	16
HDT	RK-PCR	16	1024
	RK-ELM	32	256
	RBF-SVM	128	64

4. RESULTS AND DISCUSSION

Figure 4 shows paddy growth stages detection from time series EVI profile using (a) Sakamoto algorithm, (b) Kania algorithm, and (c) our HDT algorithm in case of segment 321774203 located in Karawang district, where blue line and green line indicate LSWI and EVI profile respectively, and paddy growth stages indicated by index 1, 2, and 3 on green line. To compare visually, dates in this figure were overlaid with dates collected from field campaign indicated by three black dot lines. The comparison of all samples in 50 segments (which total 124 times of observation) were evaluated using adjusted confusion matrix shown in table 5, 6, and 7, and total accuracy are 89.51%, 93.75%, and 94.74% respectively. They shown that our proposed algorithm has higher confidence for detecting paddy growth stages than previous studies. In case of [9] algorithm (table 7), although the accuracy looks higher than [8], but actually only 25% can be detected from data samples, and the rest of 75% are defined as an unidentified. Since its algorithm was limited for detecting some time periods, so it was unable to detect all the time of MODIS data. In addition, since it also did not use smoothing process on constructing EVI profile, as consequence, the detection results were not stable. Meanwhile, harvesting date defined by previous studies was too short and specific in time scale, therefore this date would be found rarely among a series of 8-day composite MODIS images.

Since the accuracy of Sakamoto and HDT algorithm have high confidence for detecting paddy growth stages, so all data samples labeled by these algorithms can be considered as ground reference data for building the prediction models correspond to six-bands spectral of MODIS data in time invariant. We assumed that MODIS data used in learning process are free of cloud, therefore we constrained on data samples with spectral value of blue band less than 0.2. After calibration process for defining parameter γ and C , and learning process through 10-rounds random bootstrap re-

sampling method to obtain more variety on hypothesis models, the best model for each classifier method is defined as the one, which has the highest kappa coefficient during testing. Table 8 shows the best learning results during training, validation, and testing for each base learner. Our proposed method has much better accuracy than Sakamoto, and all base learners (RK-PCR, RK-ELM, and RBF-SVM) have competitive accuracy in testing. It proves that our prediction model in time invariant has a good deal with direct MODIS data in spectral-based, and has a more general prediction model for single temporal resolution of MODIS data. In addition, learning in testing can give better accuracy than learning in training, even though number of training data is much less than testing. It means that our constructed models using kernel-based learner in time invariant manner have good deal with direct spectral-based of MODIS data, and have general prediction model for single temporal resolution of MODIS data.

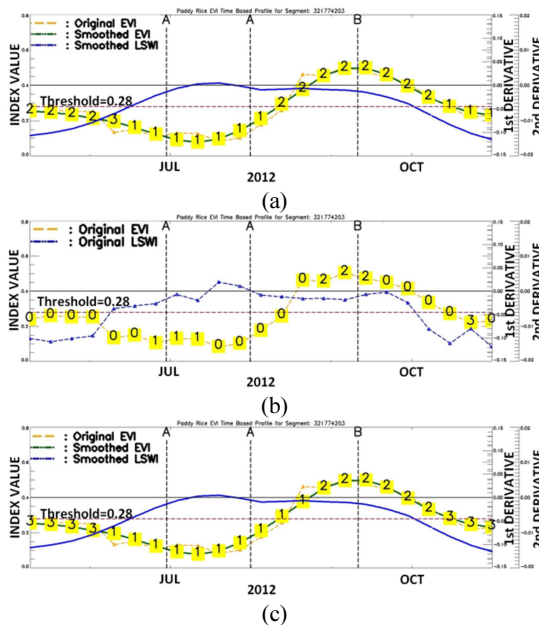


Figure 4: Paddy Growth Stages Detection In Case Of Segment 321774203, Karawang District (a) Sakamoto Algorithm [8], (b) Kania Algorithm [9], (c) A Heuristic Decision Tree

Table 5: Confusion Matrix For HDT algorithm

		Field campaign		
		A	B	C
HDT	1	39	2	4
	2	0	57	10
	3	1	0	21

Table 6: Confusion Matrix For Sakamoto Algorithm [8]

		Field campaign		
		A	C	B
Sakamoto	1	54		2
	2		11	
	3			57

Table 7: Confusion Matrix For Kania Algorithm [9]

		Field campaign		
		A	C	B
Kania	1	13		0
	2		2	
	3			17
	Unidentified	50		42

Table 8: Learning results

Data source	Base Learner	Kappa		
		Training	Validation	Testing
Sakamoto [9]	RK-PCR	0.7099	0.7022	0.6845
	RK-ELM	0.6963	0.6841	0.6825
	RBF-SVM	0.7256	0.6841	0.6949
HDT	RK-PCR	0.8793	0.8753	0.8485
	RK-ELM	0.8660	0.8727	0.8449
	RBF-SVM	0.8963	0.8518	0.8252

5. CONCLUSIONS

In this study, we proposed a new algorithm for detecting paddy growth stages from time series LSWI and EVI profile derived from MODIS data. Even though initially we used multi temporal time series MODIS data, we pursue a general model, which can be applied for any given time. Instead of relying one time series data, we develop the extraction of spectral data. After validating with ground-referenced data, we use all the samples labeled as in [8] and [9] for comparison purpose.

Our proposed method gives a prediction model in time invariant manner by introducing three kernel-based learners (RK-PCR, RK-ELM, and RBF-SVM). The results show that our proposed method give significantly better accuracy than the previous methods [8] and [9]. All kernel-based learners have good accuracy (more than 80%) in testing and have a slice difference accuracy than in training, even

though the number of data during the training is far less than during the testing. We successfully build prediction models for detecting three dates of paddy growth stage in time invariant manner using only single temporal resolution of MODIS data, and advocating the application of the general prediction model which can give more reliable, faster, and cheaper computation cost requirement (in term of processing load and memory) for real prediction model using MODIS remote sensing data.

However, since our prediction models are constructed based on cloud-free MODIS data, this model may not work for certain cloudy MODIS. In future study, it is necessary to consider an effective way for cloud removal to improve the accuracy and generalization capability of the prediction model.

REFERENCES:

- [1] S. Mulyono, M. Ivan Fanany, T. Basaruddin, "Genetic Algorithm Based New Sequence Principal Component Regression (NS-PCR) For Feature Selection And Yield Prediction Using Hyperspectral Remote Sensing Data", *International Geosciences and Remote Sensing Symposium*, 2012
- [2] S. Mulyono, M. Ivan Fanany, T. Basaruddin, "A Paddy Growth Stages Classification Using MODIS Remote Sensing Images with Balanced Branches Support Vector Machines", *International Conference on Advanced Computer Science and Information Systems*, 2012
- [3] Wang Lin, Zhang Fu-cun, Jing Yuan-shu, Jiang Xiao-dong, Yang Shen-bin, Han Xiao-mei, "Multi-temporal detection of rice phenological stages using canopy spectrum", *ScienceDirect, Rice Science*, 2014, 21(2): 108-115
- [4] Xiangming Xiao, T. Stephen Boles, Jiyuan Liu, Dafang Zhuang, Steve Froking, Changsheng Li, William Salas, Berrien Moore, "Mapping paddy rice agriculture in southern China using multi-temporal MODIS images", *Remote Sensing of Environment* 95 (2005) 480-492
- [5] Xiangming Xiao, Stephen Boles, Steve Froking, Changsheng Li, Jagadeesh Y. Babu, William Salas, Berrien Moore, "Mapping paddy rice agriculture in South and Southern Asia using multi-temporal MODIS images", *Remote Sensing of Environment* 100 (2006) 96-113
- [6] Dailing Peng, Alfredo R. Huete, Jingfeng Huang, Fuming Wang, Huasheng Sun, "Detection and estimation of mixed paddy rice cropping patterns with MODIS data", *International Journal of Applied Earth Observation and Geoinformation* 13 (2011) 13 – 23
- [7] S. Jeong, S. Kang, K. Jang, H. Lee, S. Hong, D. Ko, "Development of Variable Threshold Models for detection of irrigated paddy rice fields and irrigation timing in heterogeneous land cover", *Agricultural Water Management* 115 (2012) 83-91
- [8] Toshihiro Sakamoto, Masayuki Yokozawa, Hitoshi Toritani, Michio Shibayama, Naoki Ishitsuka, Hiroyuki Ohno, "A crop phenology detection method using time-series MODIS data", *Elsevier Remote sensing of environment* 96, 2005, 366 – 374
- [9] Dewi Kania Sari, Ishak H. Ismullah, Widyo N. Sulasdi & Agung B. Harto, "Detecting rice phenology in paddy fields with complex cropping pattern using time series MODIS data - A case study of northern part of West Java Indonesia", *ITB Journal Science Vol. 42 A, No. 2, 2010, 91-106*
- [10] Elodie Vintrou, Agnès Bégué, Christian Baron, Alexandre Saad, Danny Lo Seen, and Seydou B. Traoré, "A Comparative Study on Satellite- and Model-Based Crop Phenology in West Africa", *Remote Sensing Journal* 2014, 6, 1367-1389; doi:10.3390/rs6021367
- [11] Gillian L. Galford, John F. Mustard, Jerry Melillo, Aline Gendrin, Carlos C. Cerri, Carlos E.P. Cerri, "Wavelet analysis of MODIS time series to detect expansion and intensification of row-crop agriculture in Brazil", *Remote sensing of environment* 112, 2008, 576-587
- [12] Boonyasith Khobkhun, Akara Prayote, Preesan Rakwatin, and Natasha Dejdumrong, "Rice phenology monitoring using PIA time series MODIS imagery", *10th International conference computer graphics, Imaging and visualization*, 2013
- [13] Rick Archibald and George Fann, "Feature Selection and Classification of Hyperspectral Images With Support Vector Machines", *IEEE Geoscience and Remote Sensing Letter*, vol.4, No.4, October 2007
- [14] Chih-Wei Hsu, Chih-Chung Chang, and Chih-Jen Lin, "A Practical Guide to Support Vector Classification", *Software available at <http://www.csie.ntu.edu.tw/~cjlin>*, last updated April 15, 2010



- [15] Gustavo Camps-Valls, and Lorenzo Bruzzone, "Kernel Based Method for Hyperspectral Image Classification", *IEEE Trans. on Geosci. and RS*, Vol. 43, no. 6, June 2005
- [16] Guang-bin Huang, Qin-Yu Zhu, Chee-Kheong Siew, "Extreme learning machine: Theory and applications", *Elsevier Neurocomputing* 70 (2006) 489–501
- [17] Arthur E. Hoerl and Robert W. Kennard, "Ridge regression: biased estimation for nonorthogonal problem", *Technometrics* 12(1):55-67
- [18] S. Uchida, "Monitoring of Planting Paddy Rice with Complex Cropping Pattern in the Tropical Humid Climate Region Using LANDSAT and MODIS data - A Case of West Java, Indonesia", *International Archives of the Photogrammetry, Remote Sensing and Spatial Information Science, Volume XXXVIII, Part 8, Kyoto Japan 2010*
- [19] Peter M. Atkinson, C. Jeganathan, Jadu Dash, Clement Atzberger, "Inter-comparison of four models for smoothing satellite sensor time-series data to estimate vegetation phenology", *Remote Sensing of Environment* 123 (2012) 400–417
- [20] N.T. Son, C.F. Chen, C.R. Cru, "Mapping Major Cropping Patterns in Southeast Asia from MODIS Data using Wavelet Transform and Artificial Neural Networks", *International Archives of the Photogrammetry, Remote Sensing and Spatial Information Sciences, Volume XXXIX-B3, 2012 XXII ISPRS Congress, 25 August – 01 September 2012, Melbourne, Australia*
- [21] N.T. Son, Chi-Farn Chen, Cheng-Ru Chen, Huynh-Ngoc Duc, Ly-Yu Chang, "A Phenology-Based Classification of Time-Series MODIS Data for Rice Crop Monitoring in Mekong Delta, Vietnam", *Remote Sensing Open Access* 2014, 6, 135-156; doi:10.3390/rs6010135
- [22] Jianwen Luo, Kui Ying, Jing Bai, "Savitzky–Golay smoothing and differentiation filter for even number data", *Elsevier Signal Processing* 85 (2005) 1429–1434